Free Radical Biology and Medicine 205 (2023) 188–201

Contents lists available at ScienceDirect

Free Radical Biology and Medicine

journal homepage: www.elsevier.com/locate/freeradbiomed

Co-administration of angiotensin II and simvastatin triggers kidney injury upon heme oxygenase-1 deficiency

Aleksandra Kopacz [a,*], Damian Klóska [a,b], Dominik Cysewski [c,d], Izabela Kraszewska [a], Karolina Przepiórska [e,f], Małgorzata Lenartowicz [e], Agnieszka Łoboda [a], Anna Grochot-Przęczek [a], Witold Nowak [a], Alicja Józkowicz [a], Aleksandra Piechota-Polańczyk [a,**]

[a] Department of Medical Biotechnology, Faculty of Biochemistry, Biophysics and Biotechnology, Jagiellonian University, Kraków, Poland
[b] Molecular Mechanisms of Diseases Laboratory, Małopolska Centre of Biotechnology, Jagiellonian University, Kraków, Poland
[c] Mass Spectrometry Laboratory, Institute of Biochemistry and Biophysics, Polish Academy of Sciences, Warszawa, Poland
[d] Clinical Research Centre, Medical University of Białystok, Białystok, Poland
[e] Laboratory of Genetics and Evolution, Institute of Zoology and Biomedical Research, Jagiellonian University, Kraków, Poland
[f] Laboratory of Neuropharmacology and Epigenetics, Department of Pharmacology, Maj Institute of Pharmacology, Polish Academy of Sciences, Kraków, Poland

A B S T R A C T

Kidneys are pivotal organ in iron redistribution and can be severely damaged in the course of hemolysis. In our previous studies, we observed that induction of hypertension with angiotensin II (Ang II) combined with simvastatin administration results in a high mortality rate or the appearance of signs of kidney failure in heme oxygenase-1 knockout (HO-1 KO) mice. Here, we aimed to address the mechanisms underlying this effect, focusing on heme and iron metabolism.

We show that HO-1 deficiency leads to iron accumulation in the renal cortex. Higher mortality of Ang II and simvastatin-treated HO-1 KO mice coincides with increased iron accumulation and the upregulation of mucin-1 in the proximal convoluted tubules. *In vitro* studies showed that mucin-1 hampers heme- and iron-related oxidative stress through the sialic acid residues. In parallel, knock-down of HO-1 induces the glutathione pathway in an NRF2-depedent manner, which likely protects against heme-induced toxicity.

To sum up, we showed that heme degradation during heme overload is not solely dependent on HO-1 enzymatic activity, but can be modulated by the glutathione pathway. We also identified mucin-1 as a novel redox regulator. The results suggest that hypertensive patients with less active *HMOX1* alleles may be at higher risk of kidney injury after statin treatment.

1. Introduction

Heme is a critical molecule for living organisms. It constitutes the prosthetic groups of hemoproteins, essential for the transport and storage of oxygen and for energy generation. Heme also affects gene expression by direct regulation of several transcription factors and repressors or by influencing miRNA processing [1]. At the same time, its overabundance – caused by extracellular overload, enhanced synthesis, breakdown of hemoproteins or impaired heme degradation – is detrimental to cells [2]. This Janus-face nature of heme requires fine-tuned regulatory mechanisms. Heme must be degraded or rapidly sequestered by heme binding proteins [1]. Most commonly, heme overload is triggered by increased red blood cell hemolysis or rhabdomyolysis (due to severe muscle injury) [3]. Importantly, despite not being the primary cause, the kidneys take the brunt of the damage. Hemolysis leads to the accumulation of iron in the tubules [4] and rhabdomyolysis is accompanied by acute kidney injury [5].

Heme oxygenase-1 (HO-1, encoded by *HMOX1* gene) is an inducible enzyme that degrades heme into ferrous ions, carbon monoxide and biliverdin. HO-1, regulated by nuclear factor erythroid 2–related factor 2 (NRF2) transcription factor, is known to have antioxidant and anti-inflammatory properties and plays a pivotal role in maintaining kidney homeostasis [3,6–8]. Lack of HO-1 results in delayed kidney maturation and impaired iron detoxification in neonatal mice [9,10]. The level of HO-1 in the kidney increases significantly in disease conditions, and HO-1 deficiency exacerbates kidney dysfunction [3]. HO-1 KO mice are especially vulnerable to rhabdomyolysis, where the acute kidney insufficiency-related mortality reaches 100% [11].

* Corresponding author.
** Corresponding author.
E-mail addresses: aleksandra.kopacz@uj.edu.pl (A. Kopacz), aleksandra.piechota-polanczyk@uj.edu.pl (A. Piechota-Polańczyk).

https://doi.org/10.1016/j.freeradbiomed.2023.05.018
Received 3 May 2023; Accepted 15 May 2023
Available online 10 June 2023

Interestingly, although HO-1 is the only mammalian inducible heme-degrading enzyme [12], the lack of its activity does not trigger significant upregulation of constitutive heme oxygenase 2 (HO-2) and does not affect total intracellular heme content [13–15], suggesting the existence of other, non-enzymatic, mechanism of its degradation. Indeed, the occurrence of hydrogen peroxide (H_2O_2)-induced heme degradation is widely recognized *in vitro* [16], but *in vivo* it is rather overlooked, with some reports linking it to heme degradation in red blood cells [17]. Importantly, such a reaction occurs at the membrane level [18] and requires the glutathione system for detoxification [16,19]. In accordance, glutathione-related pathways are upregulated in response to hemin in HO-1 deficient cells [13] and play a pivotal role in protecting against kidney injury [20]. On the other hand, glutathione can efficiently form adducts with heme [21,22] and transition metals [23,24], which could also represent a way of detoxification and cell protection.

This research was undertaken as a continuation of our previous work, in which we aimed to address the role of lipid-lowering statin (simvastatin) in the development of abdominal aortic aneurysm (AAA) in HO-1-deficient mice. Statins are inhibitors of 3-hydroxy-3-methylglutaryl-coenzyme A reductase and thus, bearing the lipid lowering capacity, are widely used in the treatment of cardiovascular diseases, including AAA. We were intrigued by the preliminary observation of enhanced mortality in HO-1-deficient mice administered with simvastatin upon induction of hypertension with angiotensin II (Ang II). It was accompanied by severe kidney failure. Based on available literature data showing that statins can cause muscle damage and thus increase the level of circulating hemoproteins [25], and considering the importance of kidney in the iron homeostasis [3], along with the susceptibility of HO-1 KO mice to rhabdomyolysis, we suspect that the heme and iron abnormalities may be the primary trigger of the kidney injury. Here, our aim was to verify this supposition.

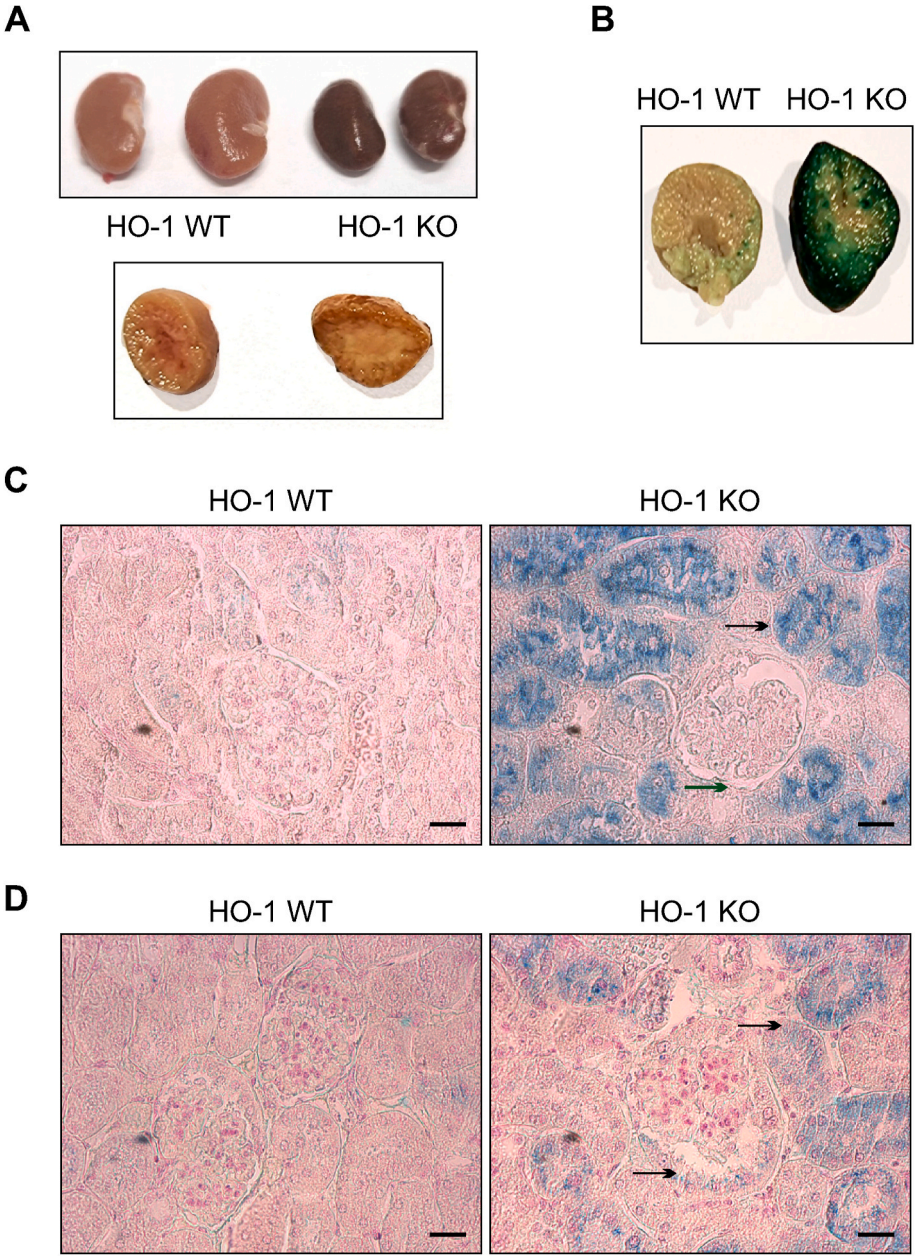

Fig. 1. HO-1 deficiency triggers iron accumulation in the renal cortex. A) kidney morphology (upper panel) and its cross-section (bottom panel) in 12-month-old HO-1 WT and KO mice; B) whole-mount iron detection by Prussian blue staining in 12-month-old HO-1 WT and KO mice; C-D) iron detection by Prussian blue staining in (C) 12- and (D) 6-month-old HO-1 WT and KO mice; iron deposits stained in blue; representative images, scale bar 50 μm.

2. Results

2.1. Deposition of iron in the renal cortex and higher susceptibility of HO-1-deficient kidneys to acute injury

Previous studies have reported the existence of microscopic iron deposition in the kidneys upon HO-1 abrogation [10,26]. In accordance, macroscopically, we observed browning of the kidneys in 12-month-old HO-1 KO mice (Fig. 1A). The color alterations localized only to the cortex (Fig. 1A, bottom panel) and proved to be Prussian blue-positive (Fig. 1B), clearly corroborating the increased iron deposition in HO-1 KO mice. The inclusions were mostly present in the proximal tubules (Fig. 1C). In younger, 6-month-old mice iron deposition was also present; however, the level of ferric ions was notably lower in the tubules and epithelial cells lining Bowman capsules start to accumulate iron (Fig. 1D).

In our previous study, we focused on establishing the role of statins (namely simvastatin) in the development of abdominal aortic aneurysm (AAA) in HO-1 deficiency. Surprisingly, we found that mice that received simvastatin along with administration of Ang II (the three-combination model) show a strong increase in mortality. The early mortality occurred approximately 3 days after Ang II infusion and was independent of aneurysm formation. The highly plausible cause of death was kidney failure, as we repeatedly observed kidney yellowing, a nephropathy caused by accumulation of bile pigments [27], products of heme metabolism. In the surviving mice, the urine was red or brown, which may be related to hematuria or occurring rhabdomyolysis [28] (Fig. 2A). Importantly, while the level of ferrous ions in the kidneys was comparable between all the inspected groups (Fig. 2B), there was a clear impact of HO-1 deficiency on the accumulation of ferric ions. Moreover, the co-treatment of HO-1 KO mice with Ang II and statin synergistically increased the non-heme ferric iron deposition (Fig. 2C). To conclude, HO-1 deficiency results in ferric iron accumulation in the renal cortex, which coincides with higher mortality in mice.

2.2. Mucin-1 accumulation accompanies kidney failure

To verify if the aforementioned symptoms may be related to renal damage, we performed Periodic Acid Schiff (PAS) staining to visualize the kidney structure (Fig. 3A). We observed thick and distinct PAS-positive rim around the glomerulus in the three-combination model. Moreover, in this group, PAS-positive material accumulated in some of

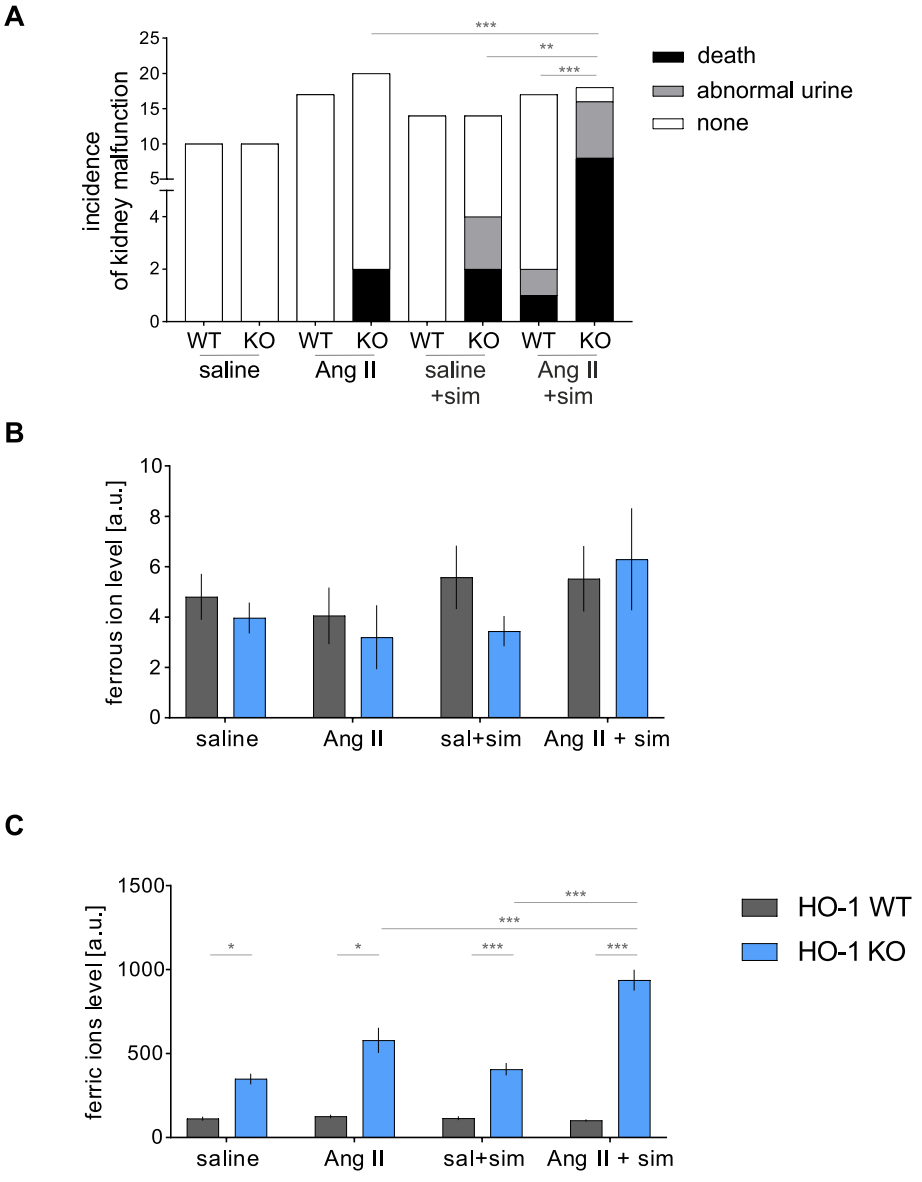

Fig. 2. Co-administration of angiotensin II and simvastatin triggers kidney injury which coincides with increase in non-heme iron. A) incidence of kidney abnormalities in 6-month-old HO-1 WT and KO mice treated with Ang II and/or simvastatin; death – death likely related to renal failure, noted by yellowing of the kidney detected on necropsy without any other anomalies; Fisher exact test; B–C) the level of heme- (B) and non-heme- (C) iron, three-way ANOVA followed by Tukey's post hoc test; *$p < 0.05$, **$p < 0.01$, ***$p < 0.001$.

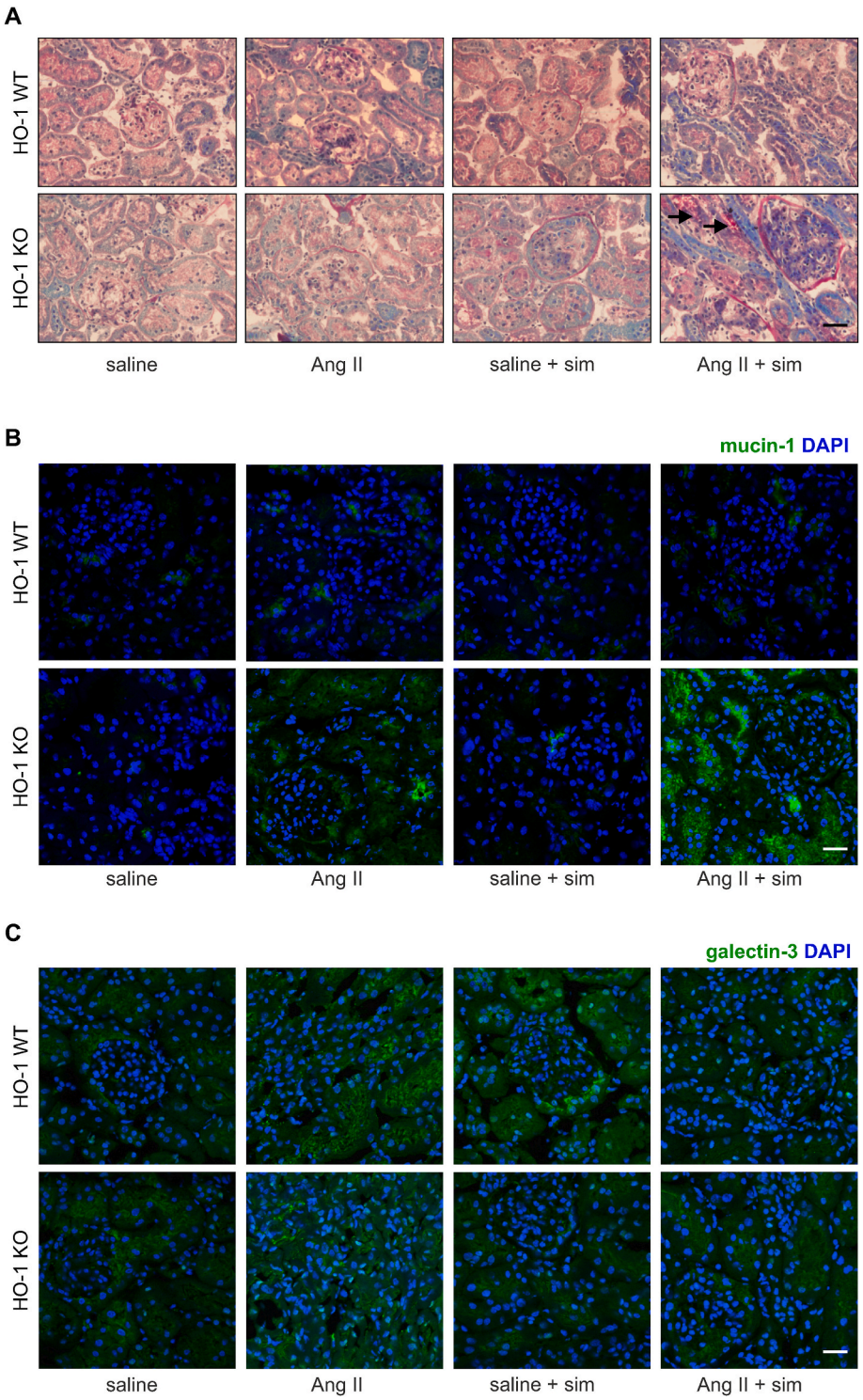

Fig. 3. Mucin-1 accumulation accompanies kidney failure. A) kidney microscopical morphology (PAS staining), in HO-1 KO mice treated with Ang II and simvastatin, representative images showing the accumulation of PAS-positive material in the proximal tubules (arrows) scale bar 25 μm; B–C) immunofluorescent staining of mucin-1 (B) and galectin-3 (C); proteins are stained in green, nuclei in blue, representative images, scale bar 25 μm.

the tubules (black arrows) and we could distinguish intensely blue staining all over the specimen. Importantly, such blue staining can be a sign of increased protein aggregation, and is observed in the cytoplasm of proximal convoluted tubular epithelial cells in renal biopsies from nephrotic syndrome patients [29]. We did not notice significant changes in the inspected groups, except for the three-combination model, where we could observe thickening of the basal membrane and possible onset of focal segmental glomerulosclerosis (Fig. 3A).

In further studies, we focused on mucin-1, which stains positively in PAS. Mucin-1 has a protective impact on the kidney [30] and can mitigate oxidative stress [31]. Indeed, immunofluorescent staining confirmed the strong expression of mucin-1 in the lumen of convoluted tubes of the Ang II + simvastatin-treated HO-1 KO mice (Fig. 3B). As mucin-1 staining pattern was unusual and the protein seemed to aggregate in the renal tubules, we decided to inspect the level and localization of its interacting protein galectin-3, that showed much more

uniform staining intensity (Fig. 3C). Noteworthy, the staining intensity of galectin-3 reflected the protein abundance assessed by mass spectrometry (Table 1).

2.3. Mucin-1 protects against hemin-related oxidative stress in the absence of HO-1

To address the functional significance of mucin-1 upregulation, we moved to *in vitro* studies. The available literature suggests that the sialic acids in mucin-1 act as potent scavengers of hydroxyl radical [31], thus we suppose that mucin-1 could protect against reactive oxygen species (ROS) in the kidneys. Indeed, we found that mucin-1 protects *HMOX1*-silenced renal tubular cells from hemin-induced oxidative stress (Fig. 4A). Furthermore, mucin-1 knock-down intensifies ferric ion-induced lipid peroxidation in HO-1 deficient cells (Fig. 4B). To address the impact of sialic acid, we used neuraminidase, which cleaves terminal sialic acids. Their removal triggered hemin-induced lipid peroxidation in HO-1-deficient cells (Fig. 4C).

Importantly, lack of mucin-1 and treatment with neuraminidase have similar outcomes, implying that the sialic acids in mucin-1 are involved in the protection against ROS. To sum up, Ang II and simvastatin-treated HO-1 KO mice upregulate mucin-1, which accumulates in the renal proximal tubules. Based on *in vitro* studies, we suppose that the increase in mucin-1 can serve as protection against heme overload-related oxidative stress.

2.4. Surviving HO-1 KO mice have higher glutathione transferase levels in the kidneys

To understand the mechanism governing the kidney dysfunction, we performed the whole proteome analysis. We could clearly distinguish a cluster of significantly upregulated proteins in Ang II + simvastatin-administered HO-1 KO animals (Fig. 5A, Supp. Fig. 1, Table 1). It mainly consisted of proteins assisting the redox homeostasis, involved in the glutathione (GSTP1, GSTA, GSTM), and thioredoxin (TXND5) systems. Moreover, there was a clear upregulation of macrophage inhibitory factor (MIF), which is involved in the tubular regeneration [32] and possess a moonlighting activity of glutathione transferase [33]. Although in the high-throughput analysis we did not include the saline + simvastatin group, we evidenced that it has no effect on the expression of the glutathione pathway (Supp. Fig. 2).

Importantly, the pathway analysis of proteins exclusively present in the three-combination model, indicated for the enrichment of 'glutathione conjugation' regulators (Reactome database, $p < 2.97e^{-7}$) and the cluster related to iron or heme binding (DAVID, $p < 4e^{-5}$). Peering closer, we could find a HO-1 deficiency-related upregulation of glutathione transferases (GSTs) and some regulators of glutathione synthesis (GCLC), whereas the levels of glutathione-degradation degrading enzymes (GPXs) were unchanged (Fig. 5B). Furthermore, the abundance of proteins related to H_2O_2 metabolism remained largely stable in all groups compared, with the exception of peroxiredoxin-1 (PRDX1) known as heme binding protein-23, which tended to increase in HO-1 KO mice, and extracellular superoxide dismutase (SOD3), which was significantly downregulated in Ang II + simvastatin-treated KO mice (Fig. 5C).

The analysis of iron or heme related proteins revealed a possible shift in iron and heme availability. While iron-binding ferritin heavy chain-1 (FTH1) and ferrochelatase (FECH) were pronouncedly upregulated upon HO-1 deficiency, NADH:ubichinon oxidoreductase (NDUC2, iron:sulfur protein) was affected both by lack of HO-1 and the used compounds. On the other hand, heme binding α-microglobulin (AMRP) was significantly downregulated by Ang II, which could enhance heme availability (Fig. 5D).

Given the significant alterations in the redox regulators, we inspected the oxidation status within the kidneys. We observed a significant increase in the level of oxidative posttranslational modifications assessed by mass spectrometry in the three-combination model (Fig. 6A). Furthermore, lipid peroxidation (assessed by appearance of

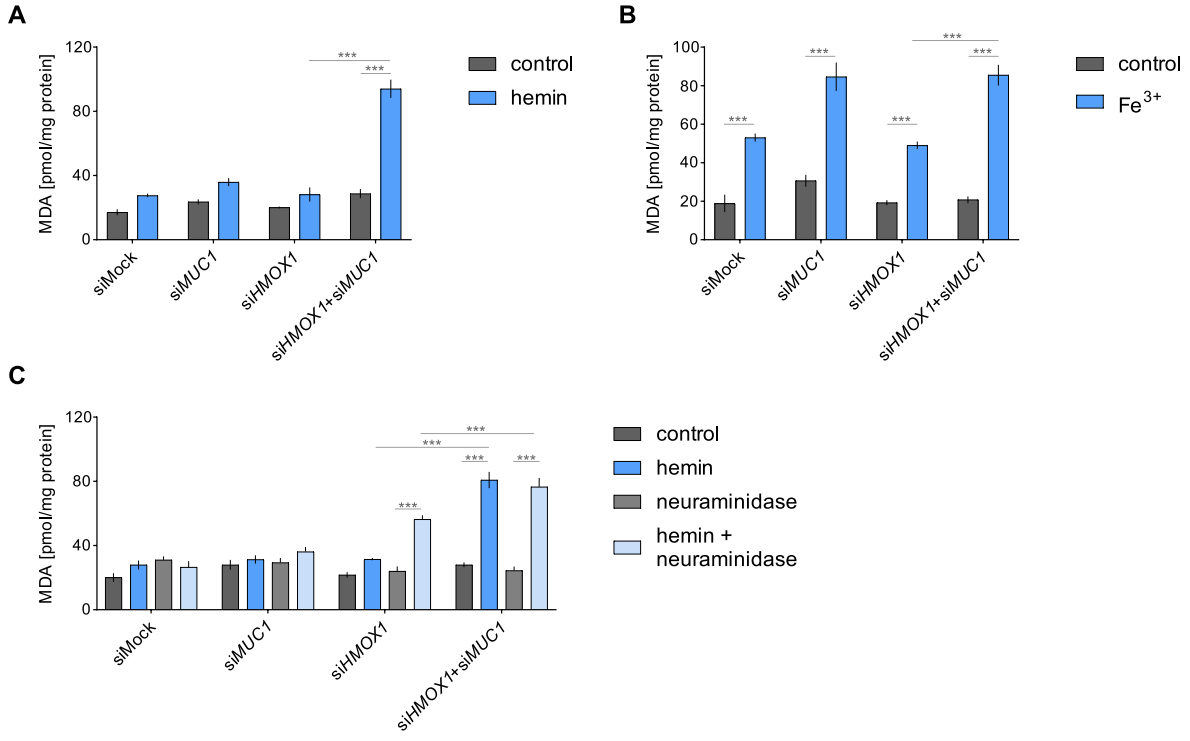

Fig. 4. Mucin-1 protects against hemin-related oxidative stress in HO-1-deficient cells. A-C) lipid peroxidation assessed by the level of thiobarbituric reactive substance (TBARS): (A) Human kidney tubular cells were transfected with siRNA targeting *HMOX1* and/or *MUC1* and then were treated with 25 μM hemin for 24 h (A) or 10 μM ferric chloride for 24 h or pre-treated with 50 mU/ml neuraminidase followed by incubation with 25 μM hemin for 24 h (C). ***$p < 0.001$; three-way ANOVA followed by Tukey's post hoc test.

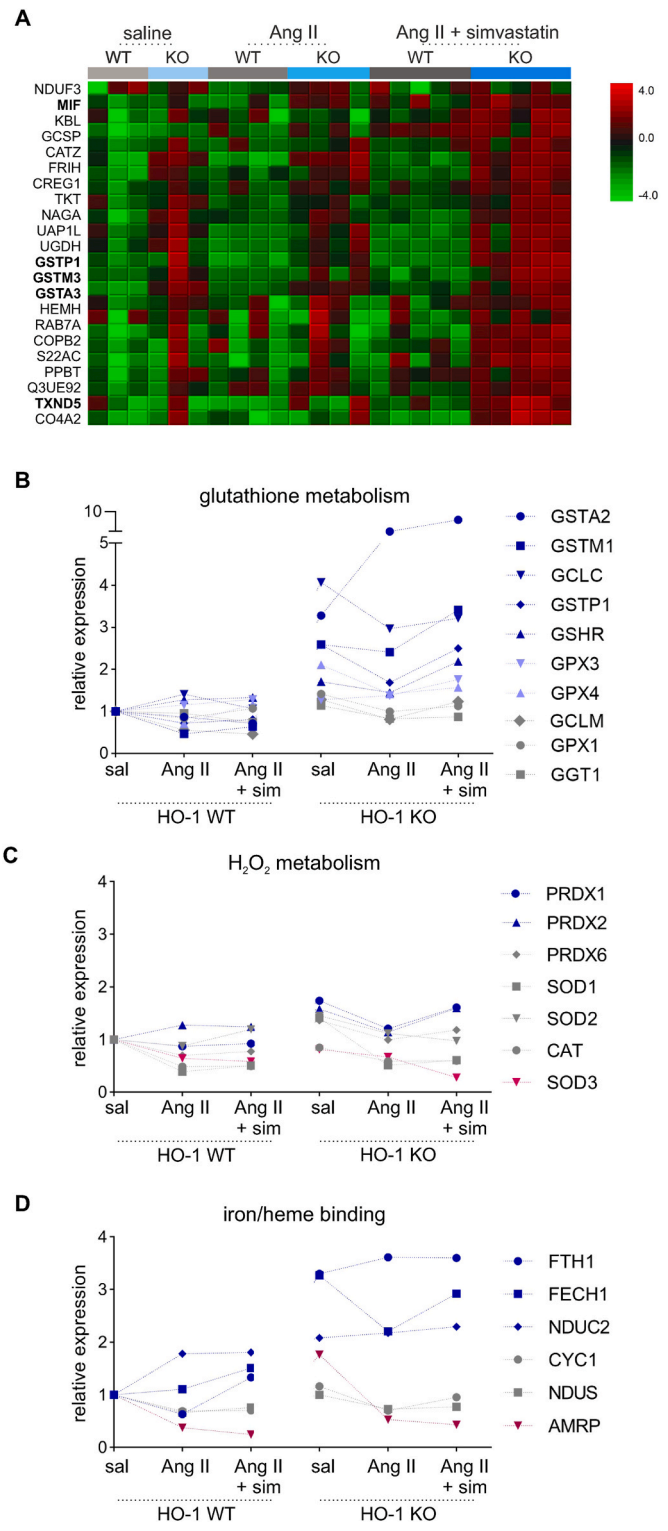

Fig. 5. Surviving HO-1 KO mice upregulate glutathione transferases. A) part of the heat-map, depicting a protein cluster significantly affected by HO-1 deficiency; FDR<1%, (B–D) level of selected proteins involved in glutathione metabolism (B), hydrogen peroxide metabolism (C) and iron/heme binding (D); data normalized to the WT saline group and represented as fold change; blue – proteins upregulated by HO-1 deficiency; grey – unchanged; red – down-regulated in some of the inspected groups. Notably, although the protein level is a discrete value, we added the connecting lines for the better legibility.

thiobarbituric acid reactive substances (Fig. 6B)) and 8-isoprostane level (Fig. 6C) showed that HO-1 deficiency irrespectively of treatment led to approximately 50% increased oxidation. Notably, while protein-bound heme level was comparable between all the inspected groups (Fig. 6D), the non-protein-bound heme (Fig. 6E) and reduced glutathione level (GSH; Fig. 6F) were increased significantly in HO-1 KO mice administered Ang II + simvastatin. The level of oxidized glutathione (GSSG) showed no difference between all analyzed groups (Fig. 6G). Altogether, we noted an appreciable increase in GSH/GSSG in the kidneys of HO-1 KO mice treated with Ang II and simvastatin (Fig. 6H). Importantly, the method employed to assess 'labile' heme likely does not discriminate between fully labile and small molecule- or peptide-conjugated heme. Therefore, we cannot rule out the possibility of the formation of glutathione-heme adducts in HO-1 KO mice administered Ang II + simvastatin [21,34], which is another way for heme detoxification. Supportively, these mice had increased protein oxidation (Fig. 6A) but not lipid peroxidation (Fig. 6B and C) in comparison to the rest of the HO-1-deficient animals.

Then we inspected how hemin stimulation *in vitro* affects glutathione-related genes upon *HMOX1*-deficiency and whether the major oxidative stress regulator NRF2, drives this protective pathway. We observed that in renal tubular cells the mRNA level of canonical NRF2 targets [35], *GCLM*, *GCLC*, *GSS*, *GSTP1* and *NQO1,* is mainly affected by heme overload in cells lacking HO-1. Importantly, this augmentation was abolished by *NFE2L2* silencing (Fig. 7).

To conclude, HO-1 deficiency does not affect the total heme level, however it promotes the oxidative state of cells. Knock-down of HO-1 induces the expression of glutathione regulators in an NRF2-dependent manner.

3. Discussion

Our study, although centered on the kidney pathophysiology, provides some important, oxidative stress- and heme-related observations. We showed that statin co-administered with Ang II induces iron accumulation in the kidney of HO-1 KO mice and may lead to nephropathy. It seems that protection against oxidative stress induced by heme overload does not rely exclusively on HO-1-mediated heme degradation. We propose that mucin-1 can act as a scavenger of ROS and thereby protect the kidney from robust oxidative damage. On the other hand, when overabundant, mucins may deteriorate kidney function [36].

Statins, which bear lipid lowering capacity, are widely used in the treatment of cardiovascular diseases, still their impact on the formation of abdominal aortic aneurysm (AAA) remains elusive. Therefore, in our previous studies, we aimed to address the role of simvastatin on the AAA formation in models of NRF2 or HO-1 deficiency.

Indeed in the model of NRF2 deficiency, we proved they protect against the aortic malformation [37]. However, in the HO-1-related studies, we did not observe the inhibitory influence of the drug in WT mice (data not shown). Moreover, as shown in this study, HO-1 KO mice were very susceptible to kidney failure, which impeded the unequivocal analysis of the impact on AAA formation. The kidney malfunction had significantly faster kinetics than the AAA formation in this strain of mice [38].

Statins possess potent antioxidant and anti-inflammatory properties [39]. However, their influence on the renal system remains controversial and the results depend on the experimental setup and patients' conditions [40]. Here, we showed that simvastatin alone did not trigger evident kidney malfunction. Only the combination of Ang II and simvastatin led to significant mortality in HO-1 KO mice probably due to kidney damage, manifested by abnormal urine production. Given that one of the major side effects proposed for statins is the muscle damage [25], we suppose that statins could cause muscle injury, and thus increase the level of circulating hemoproteins (such as myoglobin), triggering heme stress in the kidneys. However, it must be emphasized that statins alone did not affect heme and non-heme iron. In humans the

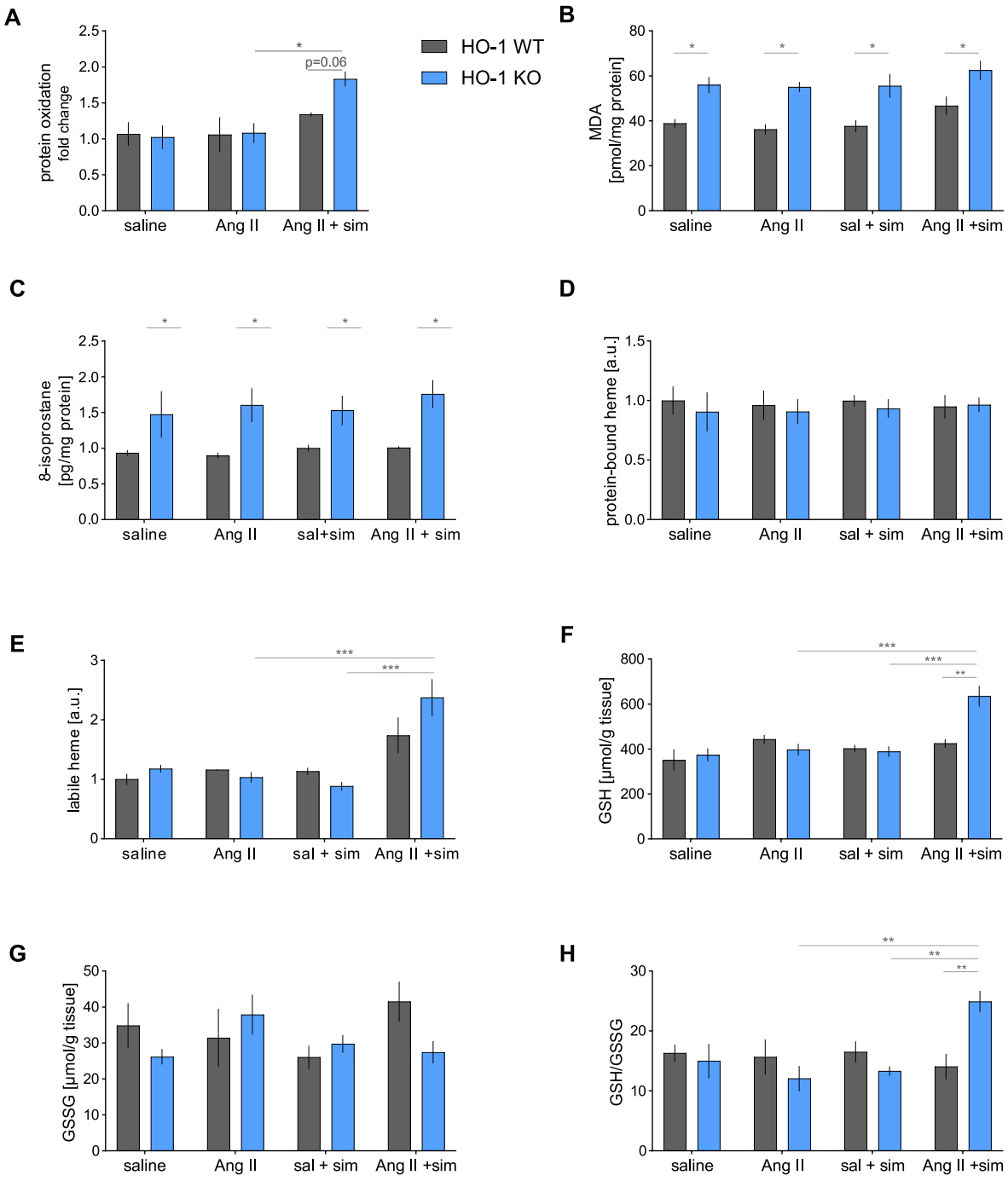

Fig. 6. HO-1 deficiency affects labile heme and reduced glutathione level. The level of (A) protein oxidation assessed by mass spectrometry, all MS-detectable oxidative modification are included, data shown as fold change of WT saline; (B–C) lipid peroxidation analyzed by (B) the measurement of thiobarbituric reactive substance (TBARS) and (C) 8-isoprostane level; (D) protein-bound and (E) labile heme content; (F) reduced and (G) oxidized glutathione; (H) GSH/GSSG ratio; *p < 0.05, **p < 0.01, ***p < 0.001; three-way ANOVA followed by Tukey's post hoc test.

adverse effects of statins are attributed to abnormal calcium homeostasis [41], which is also perturbed by Ang II [42].

One of the most commonly used models of acute kidney injury is intramuscular injection of hypertonic glycerol. In this model, HO-1 induction is the highest in the kidney and occurs 48 h after injury [11]. Supportively, even a lower dose of simvastatin than that used in our study, aggravates muscle necrosis in the mouse model of muscle dystrophy [43]. Thus, we suppose that even mild muscle lesions induced by simvastatin could account for the kidney-damaging impact of Ang II [44, 45], especially as HO-1 KO mice are extremely susceptible to rhabdomyolysis-related acute kidney injury (AKI) [11]. It is worth stressing that the characteristic manifestation of rhabdomyolysis-related tubular kidney injury is urine discoloration, which occurred in the surviving group of HO-1 KO animals treated with Ang II and statin. Moreover, kidney yellowing observed during necropsy of dead HO-1 KO mice, could be related to the accumulation of bile pigments [27], both of which are the products of non-enzymatic heme degradation [16].

The accumulation of bilirubin, which is also the product of enzymatic activity of heme oxygenases, may suggest the compensatory induction of HO-2. Indeed, the age-related impairment of HO-2 induction sensitizes older mice to acute kidney injury triggered by hemoglobin injection as evidenced by slight increase in biochemical markers of

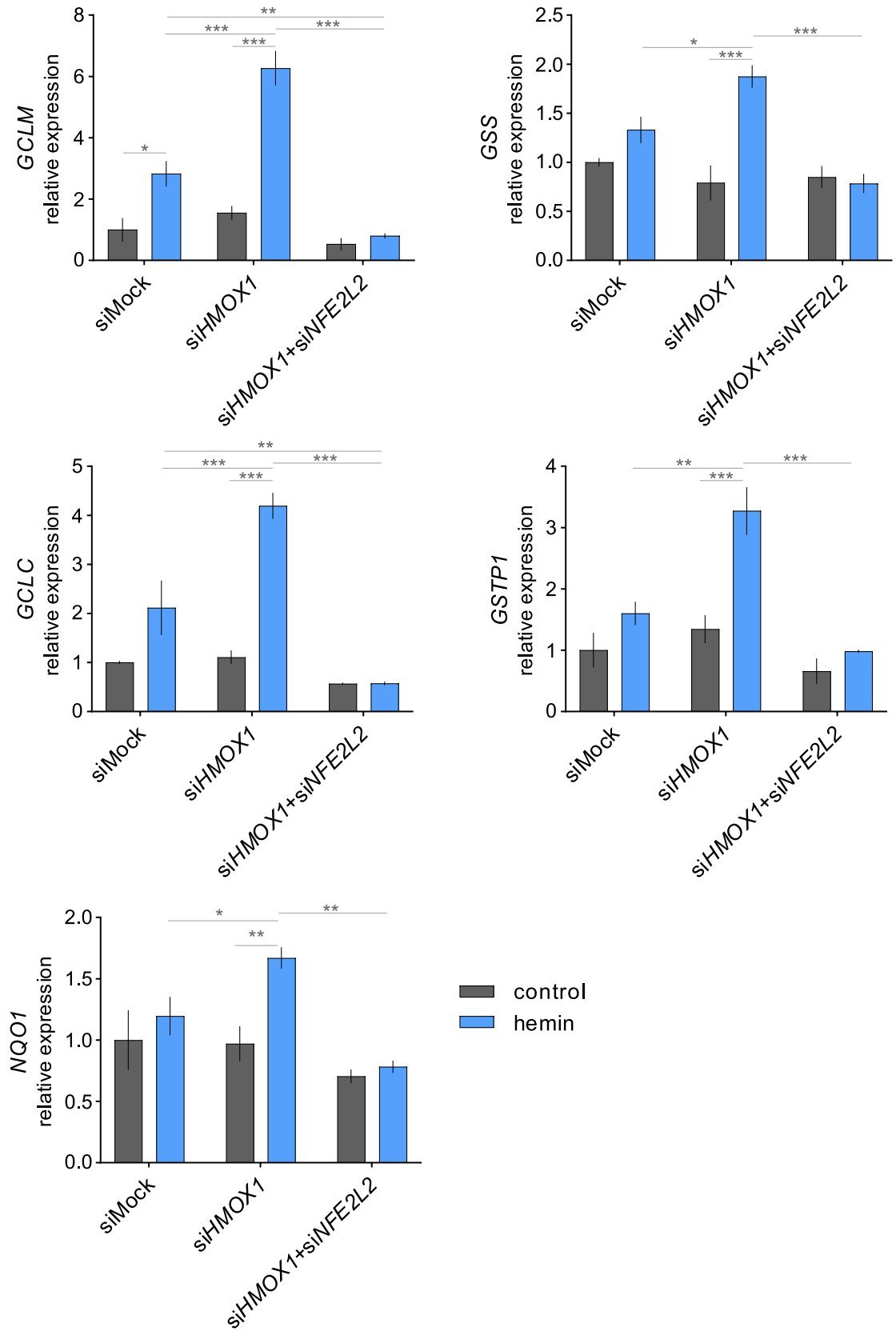

Fig. 7. NRF2 drives the upregulation of the glutathione pathway in response to heme overload. Relative expression of *GCLM*, *GCLC*, *GSS*, *GSTP1*, *NQO1*. Human kidney tubular cells were transfected with siRNA targeting *HMOX1* and/or *NFE2L2* and after 48 h were treated with 25 μM hemin for 24 h; *$p < 0.05$, three-way ANOVA followed by Tukey's post hoc test.

kidney injury and some histological changes. At the same time, in the studied model in young mice, the authors observed only 1.4 fold induction of *HMOX2*, while the induction of *HMOX1* was 4 times higher. In older animals, more susceptible to kidney injury, the induction of *HMOX1* was 20 fold, with no changes in the constitutive form [46]. In parallel, the hemin stimulation of HO-1-lacking mesenchymal stromal cells did not lead to induction of *HMOX2* [13]. The reason behind may be the scarcity of regulatory elements in the *HMOX2* promoter in comparison to *HMOX1* [47]. Moreover, we need to bear in mind that HO-1 KO, not HO-2 KO, mice are at 80% mortality risk in the heme-related models of AKI [11].

Non-enzymatic H_2O_2-dependent heme degradation *in vivo* has been studied in erythrocytes [48]. Here, in proteome profiling, we did not detect changes in the level of the majority of H_2O_2-related enzymes. In general, catalase and other H_2O_2-disposing enzymes are assumed to be protective, fine-tuning the heme degradation [17]. Among the significantly altered H_2O_2-related proteins, we could distinguish an impact of HO-1 deficiency on the level of peroxiredoxin-1 (PRDX1). Interestingly, it is also known as heme binding protein-23 [49]. Thus, PRDX1 serves two functions: cysteine-dependent peroxidase and cytosolic heme scavenger [50]. Binding heme to PRDX1 can reduce heme toxicity and degradation. Moreover, due to its cellular abundance (approximately 20 μM), PRDX1 significantly exceeds the level of heme under the basal conditions (approximately 1 μM), permitting efficient scavenging [50].

Another way of non-enzymatic heme detoxification relies on glutathione (GSH) [16,19], which is a scavenger of free heme [22]. Additionally, GSH can detoxify chemicals through direct binding or enzymatic conjugation by glutathione-*S*-transferases (GST) [51]. This seems especially relevant taking into consideration that GSTs are among the most altered proteins in HO-1 deficient kidneys in our study. GSH efficiently reacts with heme even in the presence of serum proteins; glutathione-heme complexes are present in healthy human erythrocytes and increase with hemolysis [21]. While glutathione-heme adducts have not been detected in kidneys yet, the literature documented other GSH-oxidant reactions, for example, the appearance of GSH-menadione adducts, which are exported from renal tubular cells [52].

Notably, another significantly altered protein in the HO-1 KO Ang II + simvastatin group is macrophage inhibitory factor (MIF). It is a regulator of inflammatory and immune responses, but also a moonlighting GST [33]. Moreover, it is a potent protector against acute kidney injury [32,53,54]. Still, it also emphasizes the importance of GSTs, and suggests that protective mechanisms may reach beyond the typical glutathione enzymes. Based on the detoxification capacity and the literature data, we can suspect that glutathione pathway induction was protective in our experimental setting. Nevertheless, the distinguishing factors between surviving and dead mice, and their relevance to the glutathione pathway remain to be established.

Interestingly, non-enzymatic heme degradation occurs at the cell membrane [18]. The functionality of this location has not been pinpointed, however, based on our results, we may speculate that membranous proteins are capable of harnessing the oxidative stress related to the heme degradation. Here, we confirmed that membrane-bound mucin-1 protects against lipid peroxidation, which stays in accordance with previous reports showing mucin-1 is a ROS scavenger [31]. In parallel, different subsets of mucins accumulate in the skin during rhabdomyolysis [55], and mucin-1 is a marker of chronic kidney disease in humans [56]. Analysis of the raw data of transcriptome profiling shows a 3-5-fold increase in mucin expression after acute kidney injury [57,58]. This upregulation is likely a protective mechanism, as mucin-1 knockout significantly aggravates kidney injury [59,60]. However, until now, among mucin-related mechanisms governing kidney homeostasis, the ROS-related mechanisms have not been addressed. Nevertheless, a mutation in mucin-1 resulting in a truncated, aggregation-prone protein, triggers kidney failure by clogging the tubules [30]. As in this study, mucin-1 accumulates in kidney tubules, and it likely plays a role in the deterioration of kidney function in the surviving subset of mice treated with Ang II and statin. Based on *in vitro* experiments, we propose, the ROS-harnessing properties of mucin-1 are related to sialic acids. Importantly, O-glycosylation plays a pivotal role in the protection against kidney injury [61], and the chemical decrease in sialyation results in irreversible kidney failure [62].

It still remains unidentified what triggers the expression of mucin-1 in HO-1 KO mice co-treated with Ang II and simvastatin. It could be related to oxidative stress, as proved in the airways for other subtypes of mucins [63]. Heme responsive element (TGATGCA), exactly the same as reported in the *HMOX1* promoter [64], is present in the *MUC1* promoter (−11k b.p., ATACdb), however its functional relevance in the regulation of mucin-1 gene transcription has not been elucidated yet. Moreover, the mucin-1 promoter contains multiple AP-1 binding sites, which could be relevant in its regulation during stress [65]. Conversely, mucin [66], along with NRF2 [67] regulates the expression of the cystine/glutamate transporter (*SLC7A11*), which is critical in establishing cellular glutathione levels and pivotal in preventing iron-related cell death [68], also in the kidneys [69].

In *in vitro* experiments we observed an NRF2-dependent glutathione pathway induction in heme-treated renal cells lacking HO-1. In fact genes incorporated in glutathione metabolism may be good indicators of NRF2 activation [70]. For instance, *GCLC*, *GCLM* are likely to represent direct targets of NRF2 in a variety of tissues [71,72]. Here, we established the role of NRF2 in cells treated with hemin. Such a model aimed to address the plausible impact of heme overload on renal cells rather than the influence of Ang II and simvastatin. Importantly, available data show the opposite impact of these two compounds on the NRF2 level. While Ang II downregulates NRF2 activity in renal cells [73], simvastatin upregulates NRF2 protein level in the kidney by 2-fold [74]. However, these changes are rather mild in comparison to heme-induced NRF2 upregulation [75].

Taking into account the largely overlapped phenotypes of HO-1 deficiency in mice and humans, including kidney tubular injury [76], the proper understanding of all heme degradation pathways may have a therapeutic potential. Our results shed some light on the protective mechanisms in the kidney, which may be clinically relevant given the gene polymorphism-dependent variation in HO-1 expression and enzymatic activity [77]. Interestingly, the low HO-1 activity-related polymorphisms have been associated with a higher risk for AKI after cardiac surgery [78]. Accordingly, similar conclusions were made in the cohorts of patients treated with statins [79]. Therefore, it is plausible that hypertensive patients with lower expression of *HMOX1* s may be more at risk of kidney injury after statin treatment.

4. Limitations of the study

Our results highlight the possibility that glutathione-assisted heme detoxification occurs *in vivo*. Previous studies indicated the formation of glutathione-heme adducts in the probe [34], cultured cells and isolated erythrocytes [21], but not in organs, and not in the context of HO-1 deficiency. Unfortunately, our working model largely impedes direct and unequivocal measurement of labile heme. Importantly, the method employed for the assessment of 'labile' heme likely does not discriminate between fully labile and small molecule- or peptide-conjugated heme. Therefore, in this study we refer this fraction as to non-protein-bound heme. We cannot exclude the possibility of the formation of glutathione-heme adducts, as glutathione is not precipitated with majority of typical protein precipitation methods (acid or acetone-based) [80]. However, while the glutathione upregulation coincides with the changes in the non-protein-bound heme pool, it does not with lipid peroxidation - one of the main products of iron toxicity [81]. Therefore, we may suspect that heme is somehow inactivated. It is plausible that *in vivo* experiments using glutathione precursors or synthesis inhibitor, along with the models of mucin-1 deficiency, could give us further insight into the studied processes. We hope this study will pave the way for exploration of the relevance of these pathways *in vivo*.

As this is a retrospective study, we did not fully address the origin of urine abnormalities. However, the histological changes suggest the incidence of nephrotic syndrome and myoglobinuria.

Materials and methods

Animals. This study was performed on 6- or 12-month-old male HO-$1^{-/-}$ mice (KO) [82] and their wild type littermates (WT), both on mixed C57/Bl6 × FVB background. The HO-$1^{+/-}$ breeding pairs were kindly provided by prof. Anupam Agarwal, University of Alabama of Birmingham. The genotype was verified prior to the experiment by DNA analysis. The animals were maintained under specific pathogen-free conditions in individually ventilated cages (14/10h light/dark cycle at a temperature of 22 ± 2 °C) and had free access to diet and water *ad libitum*. All experimental procedures were approved by the 2nd Institutional Animal Care and Use Committee (IACUC) in Kraków, Poland (No. 74/2016 and 110/2016) and performed in accordance with the guidelines from Directive 2010/63/EU of the European Parliament on the protection of animals used for scientific purposes.

Administration of Ang II and simvastatin. WT and HO-1 KO mice (6-month-old) were randomly divided into the following groups: (1) saline (n = 3–5), (2) angiotensin II (Ang II group, n = 5), (3) saline + simvastatin (sal + sim group, n = 5–6), and (4) angiotensin II + simvastatin (Ang II + sim group, n = 6–8). The animals were infused with Ang II (2500 ng/kg/min in saline, Sigma-Aldrich) or saline (sham group) using osmotic pumps (Alzet 2004) for up to 28 days. Simvastatin (20 mg/kg/day in saline; Sigma-Aldrich) was administered each morning *via* intragastric gavage (*i.g.*) for 7 consecutive days before osmotic pumps placement and also during the Ang II infusion for another consecutive 28 days. The detailed protocol is described in our previous papers [83,84]. During osmotic pump placement, the mice were under tribromoethanol anesthesia (250 mg/kg b.w., 1.5% solution, *i.p.*). Throughout the whole experiment the mice were on diet containing 25% fat (Supp. Fig. 3).

Cell culture. Human kidney tubular cells (HKC-8) were grown in DMEM F/12 Medium (Lonza) supplemented with Insulin Transferin-Selenium (ITS-G, Gibco) and 5% fetal bovine serum (FBS) (EURx). Cells were cultured at 37 °C in a humidified incubator in 5% CO_2 atmosphere. The cells were treated with hemin (Sigma-Aldrich), ferric chloride (Avantor Performance Materials) and neuraminidase (Sigma-Aldrich) as indicated in the figure description.

Transfection with small interfering RNA. Transfections were performed using 20 nM siRNA (Ambion) against human *HMOX1* (11056), *NFE2L2* (s9493), *MUC1* (s9067) or scrambled siRNA (siMock) (Life Technologies 4390846) using Lipofectamine™ RNAiMAX Transfection Reagent (Life Technologies) in Opti-MEM I Reduced Serum medium (Life Technologies). The experiments were performed 48 h after transfection. In case of transfections targeting multiple transcripts, the amount of siRNA was multiplied. Still the total amount of siRNA was maintained through the complementing level of scrambled siRNA.

Histological and immunofluorescent staining. The periodic acid Schiff (PAS) staining kit (ab150680, Abcam) was used to visualize mucin deposition in 10 μm OCT-frozen kidney tissue samples. The samples were stained according to the manufacturer's instructions. The Prussian blue staining for iron deposition was performed on paraffin-embedded kidney samples (8 μm) using staining kit and manufacturer instructions (Sigma-Aldrich). All samples were analyzed under a light microscope (Nikon) with NIS elements BR software (Canon) at magnifications of 100 × and 400 × .

Immunofluorescent stainings (mucin-1 and galectin-3) were done on frozen 10 μm sections of the kidney. Samples were fixed with 4% paraformaldehyde and blocked in 3% goat serum in Ca^{2+} and Mg^{2+} free PBS with 0.05% Tween-20 for mucin-1 or rabbit/mouse blocking protein from Abcam (Mouse and Rabbit Specific HRP/DAB (ABC) Detection IHC kit) for galectin-3, for 1 h at room temperature (RT). After washing in PBS, the samples were incubated overnight (4 °C) with antibodies: anti-mucin-1 (ab109185, Abcam) or anti-galectin-3 (ab209344, Abcam). On the next day, the samples were washed in PBS and incubated with secondary goat-anti-rabbit antibodies conjugated with Alexa Fluor 647 (Life Technologies) for 1 h at RT. The nuclei were counterstained with Hoechst 33342 (Sigma-Aldrich). Samples were analyzed under a meta laser scanning confocal microscope (LSM-880, Carl Zeiss) at magnification 400 × and analyzed using ImageJ software (Wayne-Rasband (NIH)).

Mass spectrometry. LC-MS measurements were performed at the at the Institute of Biochemistry and Biophysics PAS according to a modified protocol [85]. The kidneys were mechanically disrupted and with sonication (Bioruptor, set: high 30 cycles 30 s on/30 s off, 8 °C) in 500 μl of 6 M guanidine chloride, 100 mM TRIS, 10 mM TCEP, 50 mM CAA and MS-Safe Sigma protease inhibitors (MSSAFE-1VL). After centrifugation (20 min at 16,000 *g*), the supernatant was collected and the pellet was discarded. 100 μl of each sample was taken and subjected to cold acetone precipitation. Pellet was resuspended in a digestion buffer: 50 μl of 6 M urea, 100 mM ABC, 1 μg of LycC/Trypsin mix (Promega V5071), vortexed at 800 rpm at 37 °C for 4 h, then 300 μl of 25 mM ABC was added, samples were vortexed at 800 rpm at 37 °C overnight. The samples were acidified with 10 μl of 5% TFA. The resulting peptide mixture was purified at Oasis HLB 10 mg sorbent (Waters), 96-well plates, vacuum-dried, and suspended in 40 μl of 2% MeCN, 0.1% TFA. The samples were measured in an online LC-MS setup of EvosepOne (Evosep Biosystems) coupled to an Orbitrap Exploris 480 (Thermo Fisher Scientific) mass spectrometer. Peptide mixtures were loaded on Evotips C18 trap columns, according to the vendor's protocol: activation of sorbent with 0.1% FA in MeCN, 2-mine-incubation in 1-propanol, chromatographic sorbent equilibration with 0.1% FA in water; samples were loaded in 30 μl of 0.1% FA, after each step, EvoTips were centrifuged at 600 g for 1 min. Chromatographic separation was carried out at a flow rate of 500 nl/min using the 88 min (30 samples per day) performed gradient on an EV1106 analytical column (Dr. Maisch C18 AQ, 1.9 μm beads, 150 μm ID, 15 cm long, EvosepBiosystems, Odense, Denmark). Data were acquired in positive mode with a data-dependent method using the following parameters. The MS1 resolution was set to 60 000 with a normalized AGC target of 300%,auto maximum inject time, and a scan range of 350 to 1400 *m/z*. For MS2, the resolution was set to 15000 with a standard normalized AGC target, auto maximum inject time, and the top 40 precursors with an isolation window of 1.6 *m/z* considered for MS/MS analysis. Dynamic exclusion was set at 20 s with an allowed mass tolerance of ±10 ppm, with a precursor intensity threshold of 5×10^3. The precursors were fragmented in HCD mode with a normalized collision energy of 30%. The spray voltage was set to 2.1 kV, with a funnel RF level of 40 and heated capillary temperature of 275 °C.

Raw data were analyzed with PEAKS X Studio [86] (build 10.6) and searched against mouse reference proteome (Uniprot proteome IDUP000000589, 55315 protein entries), digestion: trypsin semi specific, 2 max missed cleavages, 0.1 Da MS and 0.2 Da MSMS error tolerance, fixed modification: carbamidomethylation, variable modification: PTM_PEAKS open mode, FDR 1%, common contamination databases were included. The oxidative modifications included: arginine oxidation to glutamic semialdehyde; cysteine oxidation to cysteic acid; lysine oxidation to aminoadipic semialdehyde, proline oxidation to pyroglutamic acid, tryptophan oxidation (to hydroxykynurenine, oxolactone, 2-aminotyrosine), pyroglutamate formation, tyrosine nitration, oxidation of methionine, hydroxylation, and protein carbonylation.

Proteins identified as differing groups have been analyzed in terms of belonging to individual pathways with the Reactome platform [87]. Every six groups were compared semi-quantitatively (PEAKS quant, FDR 1%) and plotted in a heatmap. Significantly changed proteins are included in Table 1. The mass spectrometry proteomics data have been deposited to the ProteomeXchange Consortium via the PRIDE repository.

Heme assessment. Briefly, a 3 mm part of the kidney or 10^5 cells were homogenized and lysed by 5 cycles of freeze-thaw. At that step, the

protein concentration was assessed by bicinchoninic acid method. The lysed proteins were precipitated by ice-cold acetone (Avantor Performance Materials) and centrifuged at 10,000 *g* for 10 min. Both the precipitate and the supernatant, after a 15-min break to allow excess acetone to evaporate, were resuspended in 2 M oxalic acid (Sigma-Aldrich) and used for further analysis according to Ref. [88]. Half of the sample volume was heated at 95 °C for 30 min leading to iron removal from heme. The fluorescence of the resultant protoporphyrin at excitation wavelength 400 nm and emission wavelength 662 nm, was assessed by the Tecan Spectra II Microplate Reader (Tecan). The endogenous protoporphyrin content was subtracted. Data were normalized to total protein concentration in each sample. This method permits distinguishing between protein-bound and labile heme (Supp. Fig. 4).

Glutathione assessment. Kidney total and oxidized glutathione were measured using a Colorimetric Glutathione Detection kit (Thermo Fisher Scientific). Briefly, kidney was homogenized in 5% 5-sulphosalicilic acid solution (Sigma-Aldrich) and total glutathione was assayed spectrophotometrically using Tecan Spectra II Microplate Reader (Tecan) following the manufacturer's instructions. Oxidized glutathione was measured in homogenized samples after glutathione masking with a 2-vinylpiridine solution (Sigma-Aldrich). The results are presented as μmol per g of tissue.

Lipid peroxidation assessment by the measurement of thiobarbituric acid reacting substances (TBARS). In brief, 3 mm fragments of kidney or 10^5 cells after treatment or transfection were washed with PBS and then 20% (w/v) trichloroacetic acid containing 0.8% (w/v) thiobarbituric acid (Sigma-Aldrich) was added to each well. The cells were scratched off to the eppendorf tubes and boiled for 30 min. After cooling to room temperature and centrifugation (350 *g*, 10 min), the absorbance of the supernatant at 535 nm and for the nonspecific turbidity at 600 nm was subtracted. The amount of malondialdehyde (MDA) equivalents was calculated using the extinction coefficient of the MDA-TBA complex ($1.56 \times 10^5\ M^{-1}\ cm^{-1}$), and the results are expressed as pmol MDA/mg protein.

8-isoprostane measurement. 8-isoprostane was measured using OxiSelect™ 8-iso-Prostaglandin F2α ELISA Kit (Cell Biolabs) according to manufacturer's protocol.

Ferrous ions analysis. For the analysis, approximately 5 mg tissue was used, which was stained with FeRhoNox-1 fluorescent imaging probe (Goryo Chemical) for 30 min. After staining, we homogenized and lysed the tissue in 10% SDS in 0.01 M HCl in isopropanol. Upon centrifugation (10,000 *g*), the supernatant fluorescence was measured (excitation - 530 nm, emission - 570 nm). The level of ferrous ions was normalized to protein concentration.

Ferric ions measurement. For the analysis, approximately 5 mg tissue was used. For ferric ions assessment, we used a modified Prussian blue staining protocol, we stained the whole tissue for 20 min in 5% potassium ferrocyanide in 10% HCl. After staining, we homogenized and lysed the tissue in 10% SDS in 0.01 M HCl in isopropanol. Upon centrifugation (10,000 *g*), the supernatant absorbance was measured at 450 nm. The results were normalized to protein concentration.

Total RNA Isolation, Reverse Transcription and Quantitative PCR. RNA from cells was isolated using Rneasy Mini kit (Qiagen). cDNA was synthesized using a High-Capacity cDNA Reverse Transcription Kit (Thermo Fisher Scientific). RT-qPCR was conducted on Step-One Plus Real-Time PCR Systems using a Power SYBR® Green PCR Master Mix according to the manufacturer's instructions (Thermo Fisher Scientific). The primer sequences are gathered in Table 2. Eukaryotic human translation elongation factor 2 (*Eef2*) was used as a reference gene. Relative gene expression was calculated using the ΔΔCt method.

Statistical analysis. Data are presented as the mean ± SEM. Depending on normality checked by the Shapiro-Wilk test, the statistical assessment was done with analysis of variance (ANOVA), followed by Tukey's post hoc test. Fisher's exact test was used to calculate the frequency of kidney abnormalities. Grubb's test was used to detect statistically significant outliers ($p < 0.05$), which were not included in the statistical analysis of the results (GraphPad Prism 9 software). $P < 0.05$ was accepted as statistically significant.

Table 2
Sequences of primers used in qPCR.

Gene	Primer sequences
h*EEF2*	F: TGAGCACACTGGCATAGAGGC R: GACATCACCAAGGGTGTGCAG;
h*GCLM*	F: TTGACATGGCCTGTTCAGTCC R: GGTTACTATTTGGTTTTACCTGTGC
h*GCLC*	F: ACAATAACTTCATTTCCCAGATTAGG R: GTATTCTTGTCCTTAAATATTGGTAC
h*GSS*	F: GAAAGGCGAACTAGTGTTGG R: AAGTCCATCTGCACAGCATA
h*GSTP1*	F: ACCAGTCCAATACCATCCTG R: TGCCTTCACATAGTCATCCTTG
h*NQO1*	F: AGGACCCTTCCGGAGTAAGA, R: CCAGGATTTGAATTCGGGCG
m*Eef-2*	F: GACATCACCAAGGGTGTGCA R: TCAGCACACTGGCATAGACC
m*Gpx4*	F: CCGATATGCTGAGTGTGGTT R: ACGCAGCCGTTCTTATCAAT
m*Gclc*	F: GGGCTGCTGTCCCAAG R: CAAGAACATCGCCTCCATTC
m*Gclm*	F: GTTGCTATAGGCACCTCTGA R: GTCAAATCTGGTGGCATCAC
mGstp1	F: CTTGTCTGTATGGGCAGCTC R: GGCCTTCACGTAGTCATTCT

Declaration of competing interest

None declared.

Acknowledgements

This work was funded by the Priority Research Area BioS under the program "Excellence Initiative – Research University" at the Jagiellonian University in Krakow. APP and AGP are members of the COST Action "Bench to bedside transition for pharmacological regulation of NRF2 in noncommunicable diseases" (CA20121). AK is supported by L'Oreal for Women in Science and the START Scholarship from the Foundation for Polish Science. The graphical abstract was prepared using Biorender.com.

Appendix A. Supplementary data

Supplementary data to this article can be found online at https://doi.org/10.1016/j.freeradbiomed.2023.05.018.

References

[1] D. Chiabrando, F. Vinchi, V. Fiorito, S. Mercurio, E. Tolosano, Heme in pathophysiology: a matter of scavenging, metabolism and trafficking across cell membranes, Front. Pharmacol. 5 (2014) 61, https://doi.org/10.3389/fphar.2014.00061.

[2] K.T. Sawicki, H. Chang, H. Ardehali, Role of Heme in Cardiovascular Physiology and Disease, J. Am. Heart Assoc.. 4 (n.d.) e001138. https://doi.org/10.1161/JAHA.114.001138.

[3] A. Grunenwald, L.T. Roumenina, M. Frimat, Heme oxygenase 1: a defensive mediator in kidney diseases, Int. J. Mol. Sci. 22 (2021) (2009), https://doi.org/10.3390/ijms22042009.

[4] I. Theurl, I. Hilgendorf, M. Nairz, P. Tymoszuk, D. Haschka, M. Asshoff, S. He, L.M. S. Gerhardt, T.A.W. Holderried, M. Seifert, S. Sopper, A.M. Fenn, A. Anzai, S. Rattik, C. McAlpine, M. Theurl, P. Wieghofer, Y. Iwamoto, G.F. Weber, N. K. Harder, B.G. Chousterman, T.L. Arvedson, M. McKee, F. Wang, O.M.D. Lutz, E. Rezoagli, J.L. Babitt, L. Berra, M. Prinz, M. Nahrendorf, G. Weiss, R. Weissleder, H.Y. Lin, F.K. Swirski, On-demand erythrocyte disposal and iron recycling requires transient macrophages in the liver, Nat. Med. 22 (2016) 945–951, https://doi.org/10.1038/nm.4146.

[5] C. Liu, K. Chi, X. Geng, Q. Hong, Z. Mao, Q. Huang, D. Liu, Y. Wang, Y. Zhang, F. Zhou, G. Cai, X. Chen, X. Sun, Exogenous biological renal support improves kidney function in mice with rhabdomyolysis-induced acute kidney injury, Front. Med. 8 (2021). https://www.frontiersin.org/articles/10.3389/fmed.2021.655787. (Accessed 26 October 2022).

[6] R.R. Starzyński, F. Canonne-Hergaux, M. Lenartowicz, W. Krzeptowski, A. Willemetz, A. Styś, J. Bierła, P. Pietrzak, T. Dziaman, P. Lipiński, Ferroportin expression in haem oxygenase 1-deficient mice, Biochem. J. 449 (2012) 69–78, https://doi.org/10.1042/BJ20121139.

[7] S. Bolisetty, A. Zarjou, A. Agarwal, Heme oxygenase 1 as a therapeutic target in acute kidney injury, Am. J. Kidney Dis. 69 (2017) 531–545, https://doi.org/10.1053/j.ajkd.2016.10.037.

[8] M. Nath, A. Agarwal, New insights into the role of heme oxygenase-1 in acute kidney injury, Kidney Res Clin Pract 39 (2020) 387–401, https://doi.org/10.23876/j.krcp.20.091.

[9] A. Bednarz, P. Lipiński, R.R. Starzyński, M. Tomczyk, W. Nowak, O. Mucha, M. Ogórek, O. Pierzchała, A. Jończy, R. Staroń, J. Śmierzchalska, Z. Rajfur, Z. Baster, A. Józkowicz, M. Lenartowicz, Role of the kidneys in the redistribution of heme-derived iron during neonatal hemolysis in mice, Sci. Rep. 9 (2019), 11102, https://doi.org/10.1038/s41598-019-47414-y.

[10] A. Bednarz, P. Lipiński, R.R. Starzyński, M. Tomczyk, I. Kraszewska, S. Herman, K. Kowalski, E. Gruca, A. Jończy, R. Mazgaj, M. Szudzik, Z. Rajfur, Z. Baster, A. Józkowicz, M. Lenartowicz, Exacerbation of neonatal hemolysis and impaired renal iron handling in heme oxygenase 1-deficient mice, Int. J. Mol. Sci. 21 (2020) 7754, https://doi.org/10.3390/ijms21207754.

[11] K.A. Nath, J.J. Haggard, A.J. Croatt, J.P. Grande, K.D. Poss, J. Alam, The indispensability of heme oxygenase-1 in protecting against acute heme protein-induced toxicity in vivo, Am. J. Pathol. 156 (2000) 1527–1535.

[12] B. Thakuri, B.D. O'Rourke, A.B. Graves, M.D. Liptak, A dynamic substrate is required for MhuD-catalyzed degradation of heme to mycobilin, Biochemistry 60 (2021) 918–928, https://doi.org/10.1021/acs.biochem.0c00892.

[13] W.N. Nowak, H. Taha, N. Kachamakova-Trojanowska, J. Stępniewski, J. A. Markiewicz, A. Kusienicka, K. Szade, A. Szade, K. Bukowska-Strakova, K. Hajduk, D. Klóska, A. Kopacz, A. Grochot-Przęczek, K. Barthenheier, C. Cauvin, J. Dulak, A. Józkowicz, Murine bone marrow mesenchymal stromal cells respond efficiently to oxidative stress despite the low level of heme oxygenases 1 and 2, Antioxidants Redox Signal. 29 (2018) 111–127, https://doi.org/10.1089/ars.2017.7097.

[14] W. Krzeptowski, P. Chudy, G. Sokołowski, M. Żukowska, A. Kusienicka, A. Seretny, A. Kalita, A. Czmoczek, J. Gubała, S. Baran, D. Klóska, M. Jeż, J. Stępniewski, K. Szade, A. Szade, A. Grochot-Przęczek, A. Józkowicz, W.N. Nowak, Proximity ligation assay detection of protein–DNA interactions—is there a link between heme oxygenase-1 and G-quadruplexes? Antioxidants 10 (2021) 94, https://doi.org/10.3390/antiox10010094.

[15] D. Klóska, A. Kopacz, A. Piechota-Polańczyk, C. Neumayer, I. Huk, J. Dulak, A. Józkowicz, A. Grochot-Przęczek, Biliverdin reductase deficiency triggers an endothelial-to-mesenchymal transition in human endothelial cells, Arch. Biochem. Biophys. 678 (2019), 108182, https://doi.org/10.1016/j.abb.2019.108182.

[16] E. Nagababu, J.M. Rifkind, Heme degradation by reactive oxygen species, Antioxidants Redox Signal. 6 (2004) 967–978, https://doi.org/10.1089/ars.2004.6.967.

[17] E. Nagababu, F.J. Chrest, J.M. Rifkind, Hydrogen-peroxide-induced heme degradation in red blood cells: the protective roles of catalase and glutathione peroxidase, Biochim. Biophys. Acta 1620 (2003) 211–217, https://doi.org/10.1016/s0304-4165(02)00537-8.

[18] E. Nagababu, J.G. Mohanty, S. Bhamidipaty, G.R. Ostera, J.M. Rifkind, Role of the membrane in the formation of heme degradation products in red blood cells, Life Sci. 86 (2010) 133–138, https://doi.org/10.1016/j.lfs.2009.11.015.

[19] H. Atamna, H. Ginsburg, Heme degradation in the presence of glutathione. A proposed mechanism to account for the high levels of non-heme iron found in the membranes of hemoglobinopathic red blood cells, J. Biol. Chem. 270 (1995) 24876–24883, https://doi.org/10.1074/jbc.270.42.24876.

[20] Y. Shang, Y.L. Siow, C.K. Isaak, K. O, Downregulation of glutathione biosynthesis contributes to oxidative stress and liver dysfunction in acute kidney injury, Oxid. Med. Cell. Longev. (2016), 9707292, https://doi.org/10.1155/2016/9707292, 2016.

[21] S.K. Georgiou-Siafis, M.K. Samiotaki, V.J. Demopoulos, G. Panayotou, A. S. Tsiftsoglou, Glutathione–hemin/hematin adduct formation to disintegrate cytotoxic oxidant hemin/hematin in human K562 cells and red blood cells' hemolysates: impact of glutathione on the hemolytic disorders and homeostasis, Antioxidants 11 (2022), https://doi.org/10.3390/antiox11101959, 1959.

[22] Y. Shviro, N. Shaklai, Glutathione as a scavenger of free hemin: a mechanism of preventing red cell membrane damage, Biochem. Pharmacol. 36 (1987) 3801–3807, https://doi.org/10.1016/0006-2952(87)90441-2.

[23] N. Ballatori, Glutathione mercaptides as transport forms of metals, Adv. Pharmacol. 27 (1994) 271–298, https://doi.org/10.1016/s1054-3589(08)61036-4.

[24] G.R. Lenz, A.E. Martell, Metal chelates of some sulfur-containing amino acids, Biochemistry 3 (1964) 745–750, https://doi.org/10.1021/bi00894a001.

[25] N. Safitri, M.F. Alaina, D.A.E. Pitaloka, R. Abdulah, A narrative review of statin-induced rhabdomyolysis: molecular mechanism, risk factors, and management, Drug Healthc. Patient Saf. 13 (2021) 211–219, https://doi.org/10.2147/DHPS.S333738.

[26] G. Kovtunovych, M.A. Eckhaus, M.C. Ghosh, H. Ollivierre-Wilson, T.A. Rouault, Dysfunction of the heme recycling system in heme oxygenase 1–deficient mice: effects on macrophage viability and tissue iron distribution, Blood 116 (2010) 6054–6062, https://doi.org/10.1182/blood-2010-03-272138.

[27] A. El Chediak, K. Janom, S.H. Koubar, Bile cast nephropathy: when the kidneys turn yellow, Renal Replacement Ther. 6 (2020) 15, https://doi.org/10.1186/s41100-020-00265-0.

[28] F.Y. Khan, Rhabdomyolysis: a review of the literature, Neth. J. Med. 67 (2009) 272–283.

[29] C.N. Gamble, Periodic acid-Schiff-light green stain to detect glomerular protein deposits by routine light microscopy, Am. J. Clin. Pathol. 63 (1975) 310–317, https://doi.org/10.1093/ajcp/63.3.310.

[30] M.M. Al-Bataineh, T.A. Sutton, R.P. Hughey, Novel roles for mucin 1 in the kidney, Curr. Opin. Nephrol. Hypertens. 26 (2017) 384–391, https://doi.org/10.1097/MNH.0000000000000350.

[31] Y. Ogasawara, T. Namai, F. Yoshino, M.-C. Lee, K. Ishii, Sialic acid is an essential moiety of mucin as a hydroxyl radical scavenger, FEBS Lett. 581 (2007) 2473–2477, https://doi.org/10.1016/j.febslet.2007.04.062.

[32] A. Ochi, D. Chen, W. Schulte, L. Leng, N. Moeckel, M. Piecychna, L. Averdunk, C. Stoppe, R. Bucala, G. Moeckel, MIF-2/D-DT enhances proximal tubular cell regeneration through SLPI- and ATF4-dependent mechanisms, Am. J. Physiol. Ren. Physiol. 313 (2017) F767–F780, https://doi.org/10.1152/ajprenal.00683.2016.

[33] M.D. Swope, H.-W. Sun, B. Klockow, P. Blake, E. Lolis, Macrophage migration inhibitory factor interactions with glutathione and S -hexylglutathione, J. Biol. Chem. 273 (1998) 14877–14884, https://doi.org/10.1074/jbc.273.24.14877.

[34] R. O'Keeffe, G.O. Latunde-Dada, Y.-L. Chen, X.L. Kong, A. Cilibrizzi, R.C. Hider, Glutathione and the intracellular labile heme pool, Biometals 34 (2021) 221–228, https://doi.org/10.1007/s10534-020-00274-w.

[35] C. Tonelli, I.I.C. Chio, D.A. Tuveson, Transcriptional regulation by Nrf2, Antioxidants Redox Signal. 29 (2018) 1727–1745, https://doi.org/10.1089/ars.2017.7342.

[36] O. Devuyst, E. Olinger, S. Weber, K.-U. Eckardt, S. Kmoch, L. Rampoldi, A. J. Bleyer, Autosomal dominant tubulointerstitial kidney disease, Nat. Rev. Dis. Prim. 5 (2019) 1–20, https://doi.org/10.1038/s41572-019-0109-9.

[37] A. Kopacz, E. Werner, A. Grochot-Przęczek, D. Klóska, K. Hajduk, C. Neumayer, A. Józkowicz, A. Piechota-Polanczyk, Simvastatin attenuates abdominal aortic aneurysm formation favoured by lack of Nrf2 transcriptional activity, Oxid. Med. Cell. Longev. (2020), 6340190, https://doi.org/10.1155/2020/6340190, 2020.

[38] A. Kopacz, D. Klóska, E. Werner, K. Hajduk, A. Grochot-Przęczek, A. Józkowicz, A. Piechota-Polańczyk, A dual role of heme oxygenase-1 in angiotensin II-induced abdominal aortic aneurysm in the normolipidemic mice, Cells 10 (2021) 163, https://doi.org/10.3390/cells10010163.

[39] A. Piechota-Polanczyk, A. Jozkowicz, W. Nowak, W. Eilenberg, C. Neumayer, T. Malinski, I. Huk, C. Brostjan, The abdominal aortic aneurysm and intraluminal thrombus: current concepts of development and treatment, Front Cardiovasc Med 2 (2015) 19, https://doi.org/10.3389/fcvm.2015.00019.

[40] A. Verdoodt, P.M. Honore, R. Jacobs, E. De Waele, V. Van Gorp, J. De Regt, H. D. Spapen, Do statins induce or protect from acute kidney injury and chronic kidney disease: an update review in, J Transl Int Med 6 (2018) 21–25, https://doi.org/10.2478/jtim-2018-0005, 2018.

[41] S. Lotteau, N. Ivarsson, Z. Yang, D. Restagno, J. Colyer, P. Hopkins, A. Weightman, K. Himori, T. Yamada, J. Bruton, D. Steele, H. Westerblad, S. Calaghan, A mechanism for statin-induced susceptibility to myopathy, JACC (J. Am. Coll. Cardiol.): Basic to Translational Science 4 (2019) 509–523, https://doi.org/10.1016/j.jacbts.2019.03.012.

[42] A. Edwards, T.L. Pallone, Mechanisms underlying angiotensin II-induced calcium oscillations, Am. J. Physiol. Ren. Physiol. 295 (2008) F568–F584, https://doi.org/10.1152/ajprenal.00107.2008.

[43] O. Mucha, P. Podkalicka, K. Kaziród, E. Samborowska, J. Dulak, A. Łoboda, Simvastatin does not alleviate muscle pathology in a mouse model of Duchenne muscular dystrophy, Skeletal Muscle 11 (2021) 21, https://doi.org/10.1186/s13395-021-00276-3.

[44] D.A. Long, K.L. Price, J. Herrera-Acosta, R.J. Johnson, How does angiotensin II cause renal injury? Hypertension 43 (2004) 722–723, https://doi.org/10.1161/01.HYP.0000120964.22281.3e.

[45] Z. Xu, W. Li, J. Han, C. Zou, W. Huang, W. Yu, X. Shan, H. Lum, X. Li, G. Liang, Angiotensin II induces kidney inflammatory injury and fibrosis through binding to myeloid differentiation protein-2 (MD2), Sci. Rep. 7 (2017), 44911, https://doi.org/10.1038/srep44911.

[46] K. Nath, J. Grande, G. Farrugia, A. Croatt, J. Belcher, R. Hebbel, G. Vercellotti, Z. Katusic, Age sensitizes the kidney to heme protein-induced acute kidney injury, Am. J. Physiol. Ren. Physiol. 304 (2012), https://doi.org/10.1152/ajprenal.00606.2012.

[47] J. Muñoz-Sánchez, M.E. Chánez-Cárdenas, A review on hemeoxygenase-2: focus on cellular protection and oxygen response, Oxid. Med. Cell. Longev. (2014), e604981, https://doi.org/10.1155/2014/604981, 2014.

[48] D. Garcia-Santos, M. Schranzhofer, M. Horvathova, M.M. Jaberi, J.A. Bogo Chies, A.D. Sheftel, P. Ponka, Heme oxygenase 1 is expressed in murine erythroid cells where it controls the level of regulatory heme, Blood 123 (2014) 2269–2277, https://doi.org/10.1182/blood-2013-04-496760.

[49] S. Hirotsu, Y. Abe, K. Okada, N. Nagahara, H. Hori, T. Nishino, T. Hakoshima, Crystal structure of a multifunctional 2-Cys peroxiredoxin heme-binding protein 23 kDa/proliferation-associated gene product, Proc. Natl. Acad. Sci. USA 96 (1999) 12333–12338, https://doi.org/10.1073/pnas.96.22.12333.

[50] Y. Watanabe, K. Ishimori, T. Uchida, Dual role of the active-center cysteine in human peroxiredoxin 1: peroxidase activity and heme binding, Biochem. Biophys. Res. Commun. 483 (2017) 930–935, https://doi.org/10.1016/j.bbrc.2017.01.034.

[51] V.I. Lushchak, Glutathione homeostasis and functions: potential targets for medical interventions, J. Amino Acids (2012), 736837, https://doi.org/10.1155/2012/736837, 2012.

[52] H.E.M.G. Haenen, P. Rogmans, J.H.M. Temmink, P.J. van Bladeren, Differential detoxification of two thioether conjugates of menadione in confluent monolayers

of rat renal proximal tubular cells, Toxicol. Vitro 8 (1994) 207–214, https://doi.org/10.1016/0887-2333(94)90184-8.
[53] Y. Du, H. Hao, H. Ma, H. Liu, Macrophage migration inhibitory factor in acute kidneyinjury, Front. Physiol. 13 (2022), 945827, https://doi.org/10.3389/fphys.2022.945827.
[54] C. Stoppe, L. Averdunk, A. Goetzenich, J. Soppert, A. Marlier, S. Kraemer, J. Vieten, M. Coburn, A. Kowark, B.-S. Kim, G. Marx, S. Rex, A. Ochi, L. Leng, G. Moeckel, A. Linkermann, O. El Bounkari, A. Zarbock, J. Bernhagen, S. Djudjaj, R. Bucala, P. Boor, The protective role of macrophage migration inhibitory factor in acute kidney injury after cardiac surgery, Sci. Transl. Med. 10 (2018), eaan4886, https://doi.org/10.1126/scitranslmed.aan4886.
[55] M.J. Rothe, R. Rivas, E. Gould, F.A. Kerdel, Scleromyxedema and severe myositis, Int. J. Dermatol. 28 (1989) 657–660, https://doi.org/10.1111/j.1365-4362.1989.tb02436.x.
[56] Z.-Y. Zhang, S. Ravassa, M. Pejchinovski, W.-Y. Yang, P. Zürbig, B. López, F.-F. Wei, L. Thijs, L. Jacobs, A. González, J.-U. Voigt, P. Verhamme, T. Kuznetsova, J. Díez, H. Mischak, J.A. Staessen, A urinary fragment of mucin-1 subunit α is a novel biomarker associated with renal dysfunction in the general population, Kidney Int Rep 2 (2017) 811–820, https://doi.org/10.1016/j.ekir.2017.03.012.
[57] Y. Kirita, H. Wu, K. Uchimura, P.C. Wilson, B.D. Humphreys, Cell profiling of mouse acute kidney injury reveals conserved cellular responses to injury, Proc. Natl. Acad. Sci. USA 117 (2020) 15874–15883, https://doi.org/10.1073/pnas.2005477117.
[58] H. Li, E.E. Dixon, H. Wu, B.D. Humphreys, Comprehensive single-cell transcriptional profiling defines shared and unique epithelial injury responses during kidney fibrosis, Cell Metabol. (2022), https://doi.org/10.1016/j.cmet.2022.09.026.
[59] M. Al-bataineh, C. Kinlough, Z. Mi, E. Jackson, R. Hughey, Mucin 1 regulates KIM-1 function following ischemic renal injury, Faseb. J. 33 (2019), https://doi.org/10.1096/fasebj.2019.33.1_supplement.lb528 lb528–lb528.
[60] M.M. Al-Bataineh, C.L. Kinlough, Z. Mi, E.K. Jackson, S.M. Mutchler, D.R. Emlet, J. A. Kellum, R.P. Hughey, KIM-1-mediated anti-inflammatory activity is preserved by MUC1 induction in the proximal tubule during ischemia-reperfusion injury, Am. J. Physiol. Ren. Physiol. 321 (2021) F135–F148, https://doi.org/10.1152/ajprenal.00127.2021.
[61] K. Song, J. Fu, J. Song, B.H. Herzog, K. Bergstrom, Y. Kondo, J.M. McDaniel, S. McGee, R. Silasi-Mansat, F. Lupu, H. Chen, H. Bagavant, L. Xia, Loss of mucin-type O-glycans impairs the integrity of the glomerular filtration barrier in the mouse kidney, J. Biol. Chem. 292 (2017) 16491–16497, https://doi.org/10.1074/jbc.M117.798512.
[62] M.S. Macauley, B.M. Arlian, C.D. Rillahan, P.-C. Pang, N. Bortell, M.C. G. Marcondes, S.M. Haslam, A. Dell, J.C. Paulson, Systemic blockade of sialylation in mice with a global inhibitor of sialyltransferases, J. Biol. Chem. 289 (2014) 35149–35158, https://doi.org/10.1074/jbc.M114.606517.
[63] K. Takeyama, K. Dabbagh, J. Jeong Shim, T. Dao-Pick, I.F. Ueki, J.A. Nadel, Oxidative stress causes mucin synthesis via transactivation of epidermal growth factor receptor: role of neutrophils, J. Immunol. 164 (2000) 1546–1552, https://doi.org/10.4049/jimmunol.164.3.1546.
[64] N.M. Inamdar, Y.I. Ahn, J. Alam, The heme-responsive element of the mouse heme oxygenase-1 gene is an extended AP-1 binding site that resembles the recognition sequences for MAF and NF-E2 transcription factors, Biochem. Biophys. Res. Commun. 221 (1996) 570–576, https://doi.org/10.1006/bbrc.1996.0637.
[65] J.Z. Zaretsky, I. Barnea, Y. Aylon, M. Gorivodsky, D.H. Wreschner, I. Keydar, MUC1 gene overexpressed in breast cancer: structure and transcriptional activity of the MUC1 promoter and role of estrogen receptor alpha (ERalpha) in regulation of the MUC1 gene expression, Mol. Cancer 5 (2006) 57, https://doi.org/10.1186/1476-4598-5-57.
[66] M. Hasegawa, H. Takahashi, H. Rajabi, M. Alam, Y. Suzuki, L. Yin, A. Tagde, T. Maeda, M. Hiraki, V.P. Sukhatme, D. Kufe, Functional interactions of the cystine/glutamate antiporter, CD44v and MUC1-C oncoprotein in triple-negative breast cancer cells, Oncotarget 7 (2016) 11756–11769, https://doi.org/10.18632/oncotarget.7598.
[67] D. Chen, O. Tavana, B. Chu, L. Erber, Y. Chen, R. Baer, W. Gu, NRF2 is a major target of ARF in p53-independent tumor suppression, Mol. Cell. 68 (2017) 224–232, https://doi.org/10.1016/j.molcel.2017.09.009, e4.
[68] D. Tang, X. Chen, R. Kang, G. Kroemer, Ferroptosis: molecular mechanisms and health implications, Cell Res. 31 (2021) 107–125, https://doi.org/10.1038/s41422-020-00441-1.
[69] Y. Ye, A. Chen, L. Li, Q. Liang, S. Wang, Q. Dong, M. Fu, Z. Lan, Y. Li, X. Liu, J.-S. Ou, L. Lu, J. Yan, Repression of the antiporter SLC7A11/glutathione/glutathione peroxidase 4 axis drives ferroptosis of vascular smooth muscle cells to facilitate vascular calcification, Kidney Int. 0 (2022), https://doi.org/10.1016/j.kint.2022.07.034.
[70] A. Raghunath, K. Sundarraj, R. Nagarajan, F. Arfuso, J. Bian, A.P. Kumar, G. Sethi, E. Perumal, Antioxidant response elements: discovery, classes, regulation and potential applications, Redox Biol. 17 (2018) 297–314, https://doi.org/10.1016/j.redox.2018.05.002.
[71] L. Leung, M. Kwong, S. Hou, C. Lee, J.Y. Chan, Deficiency of the Nrf1 and Nrf2 transcription factors results in early embryonic lethality and severe oxidative stress, J. Biol. Chem. 278 (2003) 48021–48029, https://doi.org/10.1074/jbc.M308439200.
[72] L. Chen, M. Kwong, R. Lu, D. Ginzinger, C. Lee, L. Leung, J.Y. Chan, Nrf1 is critical for redox balance and survival of liver cells during development, Mol. Cell Biol. 23 (2003) 4673–4686, https://doi.org/10.1128/MCB.23.13.4673-4686.2003.
[73] S.J. Kang, A. You, M.-K. Kwak, Suppression of Nrf2 signaling by angiotensin II in murine renal epithelial cells, Arch Pharm. Res. (Seoul) 34 (2011) 829–836, https://doi.org/10.1007/s12272-011-0517-1.
[74] Y. Zhang, S. Rong, Y. Feng, L. Zhao, J. Hong, R. Wang, W. Yuan, Simvastatin attenuates renal ischemia/reperfusion injury from oxidative stress via targeting Nrf2/HO-1 pathway, Exp. Ther. Med. 14 (2017) 4460–4466, https://doi.org/10.3892/etm.2017.5023.
[75] J.J. Boyle, M. Johns, J. Lo, A. Chiodini, N. Ambrose, P.C. Evans, J.C. Mason, D. O. Haskard, Heme induces heme oxygenase 1 via Nrf2, Arterioscler. Thromb. Vasc. Biol. 31 (2011) 2685–2691, https://doi.org/10.1161/ATVBAHA.111.225813.
[76] K. Ohta, A. Yachie, K. Fujimoto, H. Kaneda, T. Wada, T. Toma, A. Seno, Y. Kasahara, H. Yokoyama, H. Seki, S. Koizumi, Tubular injury as a cardinal pathologic feature in human heme oxygenase-1 deficiency, Am. J. Kidney Dis. 35 (2000) 863–870, https://doi.org/10.1016/s0272-6386(00)70256-3.
[77] H. Taha, K. Skrzypek, I. Guevara, A. Nigisch, S. Mustafa, A. Grochot-Przeczek, P. Ferdek, H. Was, J. Kotlinowski, M. Kozakowska, A. Balcerczyk, L. Muchova, L. Vitek, G. Weigel, J. Dulak, A. Jozkowicz, Role of heme oxygenase-1 in human endothelial cells: lesson from the promoter allelic variants, Arterioscler. Thromb. Vasc. Biol. 30 (2010) 1634–1641, https://doi.org/10.1161/ATVBAHA.110.207316.
[78] D.E. Leaf, S.C. Body, J.D. Muehlschlegel, G.M. McMahon, P. Lichtner, C.D. Collard, S.K. Shernan, A.A. Fox, S.S. Waikar, Length polymorphisms in heme oxygenase-1 and AKI after cardiac surgery, J. Am. Soc. Nephrol. 27 (2016) 3291–3297, https://doi.org/10.1681/ASN.2016010038.
[79] Y.-H. Chen, K.-L. Kuo, S.-C. Hung, C.-C. Hsu, Y.-H. Chen, D.-C. Tarng, Length polymorphism in heme oxygenase-1 and risk of CKD among patients with coronary artery disease, J. Am. Soc. Nephrol. 25 (2014) 2669–2677, https://doi.org/10.1681/ASN.2013111205.
[80] E. Błońska-Sikora, J. Oszczudlowski, Z. Witkiewicz, D. Widel, Glutathione: methods of sample preparation for chromatography and capillary electrophoresis, Chem 66 (2012) 929–942.
[81] G. Minotti, S.D. Aust, The role of iron in the initiation of lipid peroxidation, Chem. Phys. Lipids 44 (1987) 191–208, https://doi.org/10.1016/0009-3084(87)90050-8.
[82] K.D. Poss, S. Tonegawa, Heme oxygenase 1 is required for mammalian iron reutilization, Proc. Natl. Acad. Sci. U. S. A. 94 (1997) 10919–10924, https://doi.org/10.1073/pnas.94.20.10919.
[83] A. Kopacz, D. Klóska, E. Werner, K. Hajduk, A. Grochot-Przęczek, A. Józkowicz, A. Piechota-Polańczyk, A dual role of heme oxygenase-1 in angiotensin II-induced abdominal aortic aneurysm in the normolipidemic mice, Cells 10 (2021) 163, https://doi.org/10.3390/cells10010163.
[84] A. Kopacz, E. Werner, D. Kloska, K. Hajduk, J. Fichna, A. Jozkowicz, A. Piechota-Polanczyk, Nrf2 transcriptional activity in the mouse affects the physiological response to tribromoethanol, Biomed. Pharmacother. 128 (2020), 110317, https://doi.org/10.1016/j.biopha.2020.110317.
[85] H.B. Schiller, I.E. Fernandez, G. Burgstaller, C. Schaab, R.A. Scheltema, T. Schwarzmayr, T.M. Strom, O. Eickelberg, M. Mann, Time- and compartment-resolved proteome profiling of the extracellular niche in lung injury and repair, Mol. Syst. Biol. 11 (2015) 819, https://doi.org/10.15252/msb.20156123.
[86] B. Ma, K. Zhang, C. Hendrie, C. Liang, M. Li, A. Doherty-Kirby, G. Lajoie, PEAKS: powerful software for peptide de novo sequencing by tandem mass spectrometry, Rapid Commun. Mass Spectrom. 17 (2003) 2337–2342, https://doi.org/10.1002/rcm.1196.
[87] M. Gillespie, B. Jassal, R. Stephan, M. Milacic, K. Rothfels, A. Senff-Ribeiro, J. Griss, C. Sevilla, L. Matthews, C. Gong, C. Deng, T. Varusai, E. Ragueneau, Y. Haider, B. May, V. Shamovsky, J. Weiser, T. Brunson, N. Sanati, L. Beckman, X. Shao, A. Fabregat, K. Sidiropoulos, J. Murillo, G. Viteri, J. Cook, S. Shorser, G. Bader, E. Demir, C. Sander, R. Haw, G. Wu, L. Stein, H. Hermjakob, P. D'Eustachio, The reactome pathway knowledgebase 2022, Nucleic Acids Res. 50 (2022) D687–D692, https://doi.org/10.1093/nar/gkab1028.
[88] P.R. Sinclair, N. Gorman, J.M. Jacobs, Measurement of heme concentration (Chapter 8), Curr Protoc Toxicol (2001), https://doi.org/10.1002/0471140856.tx0803s00. Unit 8.3.

List of abbreviations

AAA: abdominal aortic aneurysm
AKI: acute kidney injury
Ang II: angiotensin II
GCLC: glutamate - cysteine ligase catalytic subunit
GCLM: glutamate-cysteine ligase modifier subunit
GPx: glutathione peroxidase
GSH: reduced glutathione
GSS: glutathione synthetase
GSSG: oxidized glutathione
GSTs: glutathione S-transferases
GSTA: glutathione S-transferase alpha
GSTM: glutathione S-transferase mu
GSTP1: glutathione S-transferase pi 1
H_2O_2: hydrogen peroxide
HO-1 (HMOX1): heme oxygenase 1
HO-2 (HMOX2): heme oxygenase 2
KO: knockout
MDA: malondialdehyde
MIF: macrophage inhibitory factor
MUC1: mucin 1

***NRF2** (NFE2L2):* nuclear factor erythroid 2–related factor 2
***NQO1**:* NAD(P)H quinone dehydrogenase 1
***PAS**:* Peridic-Acid Schiff
***PRDX**:* peroxiredoxin
***sal**:* saline
***sim**:* simvastatin
***TBARS**:* thiobarbituric reactive substance
***WT**:* wild-type